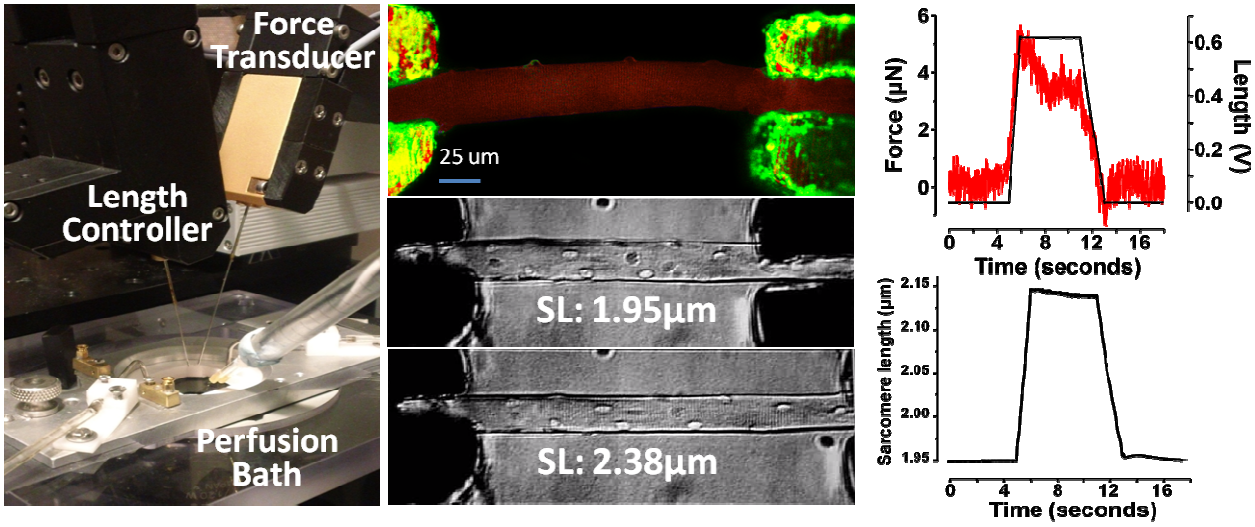

Figure S1: MuST setup. A World Precision Instruments force transducer and length controller mounted on Siskiyou folded micromanipulators over a confocal microscope equipped with an Aurora Scientific High-speed Video Sarcomere Length camera allows for the precise control of muscle length while simultaneously recording force, absolute length and sarcomere length in single enzymatically dissociated FDB myofibers.

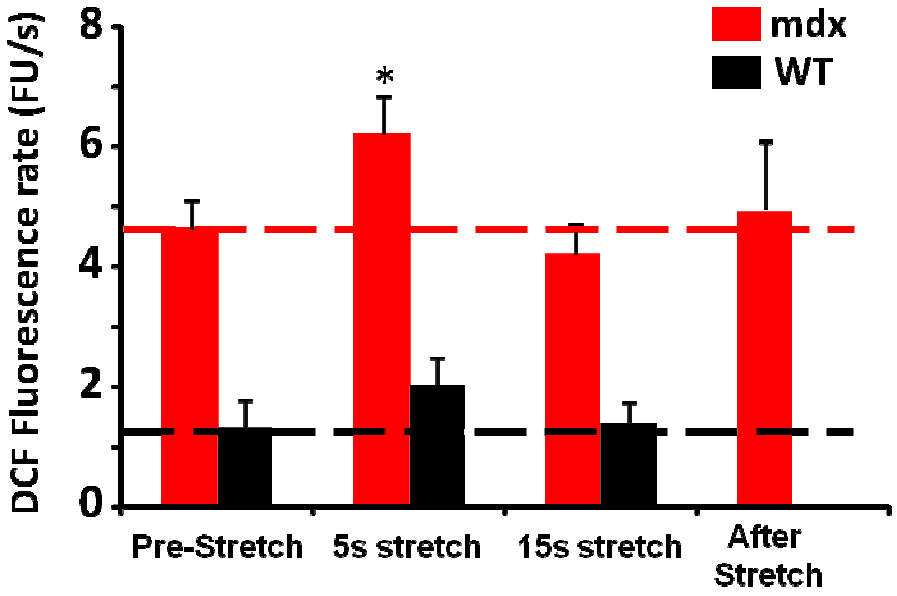

Figure S2: Acute stretch results in a transient increase in X-ROS. DCF fluorescence rate was calculated with linear least squares regression of data segments in the pre-stretch period (0-5 seconds), the stretch period (6-10 seconds) and the last 5 seconds of the stretch period (15-20 seconds). During the return to the pre-stretch length, the myofibers had significant recoil or movement artifact (20-25 seconds) which prevented analysis and this data segment was removed from the traces. The rate after return to resting stretch length was taken during the last three seconds of the 30 second run. (n=14 fibers per genotype. *; $P<0.05$ compared to pre-stretch)

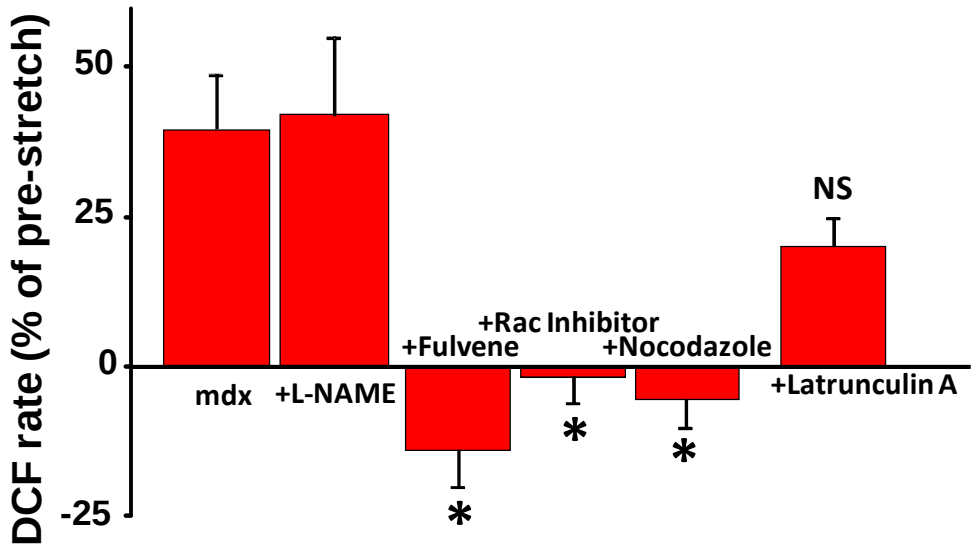

Figure S3: X-ROS signaling in dystrophic muscle fibers. X-ROS was significantly abrogated by: NOX2 inhibition (fulvene-5), Rac inhibition (Rac1 inhibitor) and microtubule destabilization (nocodazole), but not by actin destabilization (latrunculin A) or inhibition of nitric oxide synthase (L-NAME). * denotes $P<0.05$ compared to mdx.

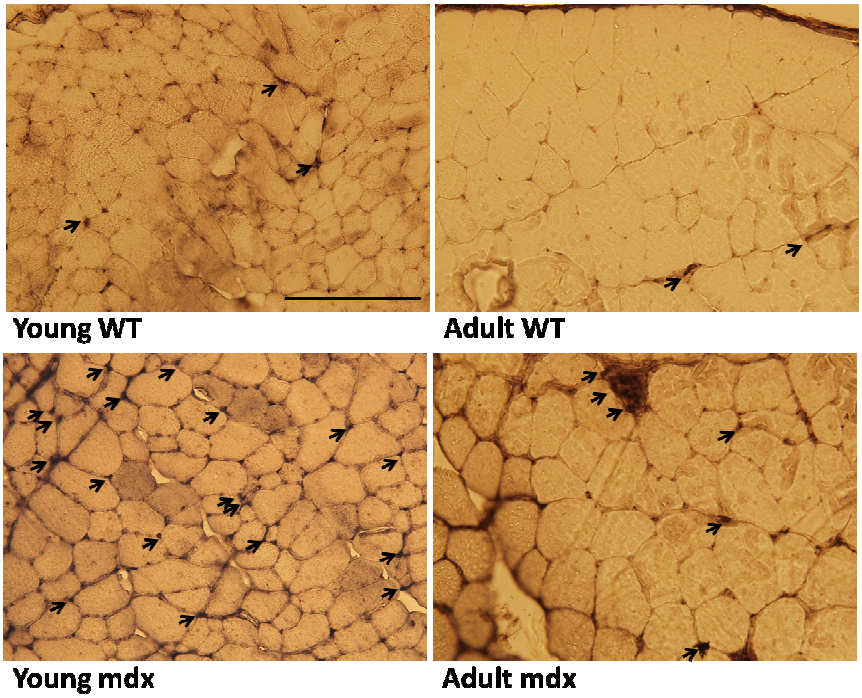

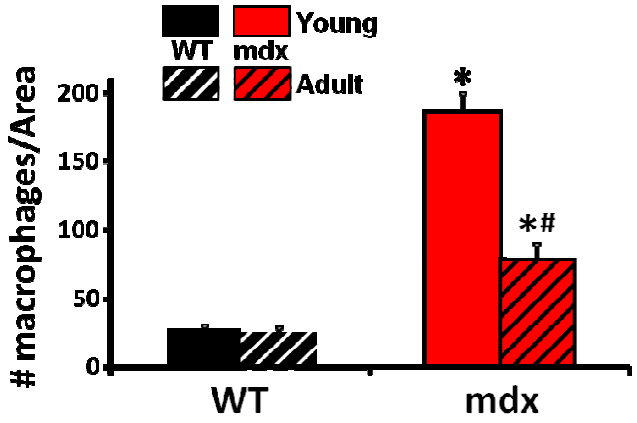

Figure S4. Macrophage infiltration in wild-type and *mdx* muscle. Tibialis anterior muscles from adult (~6 month) and young (~ 7 week) wild-type (n=3) and *mdx* (n=3) mice. Scale bar is 200 µm. *P<0.05 compared to WT. #P<0.05 compared to young.

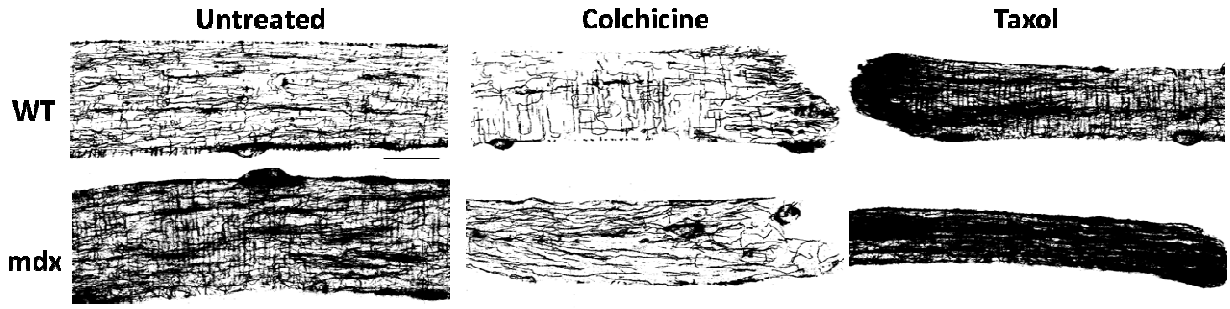

Figure S5. Binary representation of fluorescent immunolabeling images of α-tubulin. Representative images from adult WT or *mdx* FDB myofibers. Microtubule network structure was either decreased with colchicine or increased with taxol or left untreated before fixing and staining. The altered microtubule network structure in untreated *mdx* as seen here and by others (*23*) could be partially restored by expression of microdystrophin (*62*), supporting the critical role of dystrophin in microtubule network structure. Black scale bar is 20 μm.

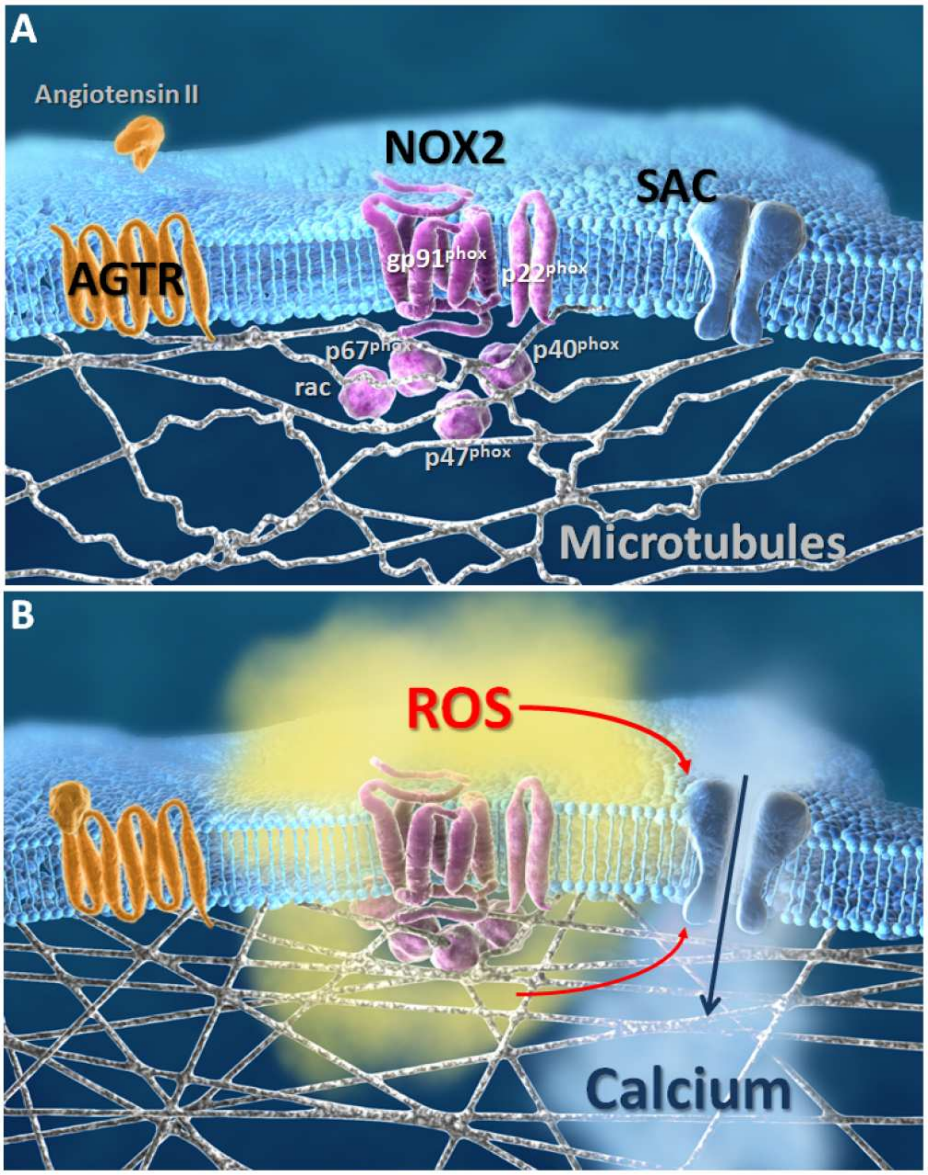

Figure S6. X-ROS and microtubules as the molecular basis of dysfunction in DMD. Simplified model of X-ROS signaling in skeletal muscle. (A) Dystrophic muscle displays increased abundance of all major components in X-ROS signaling. Activation of renin-angiotensin signaling can lead to increased density of the microtubule cytoskeleton and provide the necessary gain in signal such that a small physiologic stretch (B) leads to microtubule-dependent recruitment of the NOX2 subunits Rac, $p67^{phox}$, $p47^{phox}$ and $p40^{phox}$ and subsequent activation of NOX2. ROS can then act to enhance sarcolemmal calcium influx through stretch-activated channels.

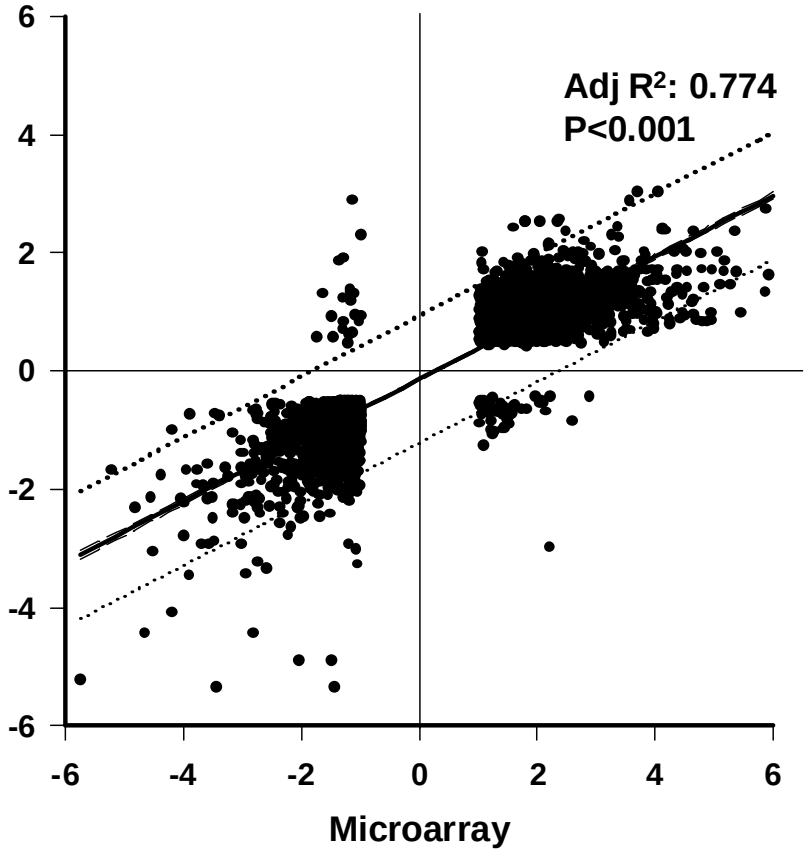

Figure S7. Regression plot of RNA-seq and microarray data demonstrates good correlation between the two sample sets. To validate the findings from our RNA-seq dataset, we examined the correlation between differentially expressed genes in DMD versus NORMAL in a microarray dataset that we had previously published (*63*). We plot the correlation between the differentially expressed genes in DMD compared to NORMAL muscle that met the 2-fold or greater cut-off and an FDR corrected p-value of 0.05 in both datasets.

Table S1. **Demographic and phenotype data for normal controls and DMD cases for RNA-seq**. Sequencing was conducted using 1 μg of total RNA isolated from each skeletal muscle biopsy samples from control subjects (NORM; n=7) and those diagnosed with Duchenne Muscular Dystrophy (DMD; n=6). Below is the information regarding the age of the subject at time of biopsy, gender and histopathological features. Samples were collected, archived and histology was performed by Dr. Eric P. Hoffman.

CNMC Phenotype Data RNA-SEQ	AGE (YRS)	GENDER	HISTOPATHOLOGY
NORM-1	15.0	Male	N/A
NORM-2	33.0	Male	N/A
NORM-3	2.0	Male	N/A
NORM-4	UNKNOWN	Male	N/A
NORM-5	UNKNOWN	Male	N/A
NORM-6	UNKNOWN	Male	N/A
NORM-7	UNKNOWN	Male	N/A
DMD-1	5.0	Male	DMD like, degeneration/regeneration, edomysial fibrosis
DMD-2	5.0	Male	Severe dystrophy, necrosis, fibrosis
DMD-3	4.0	Male	Dystrophic, degeneration/regeneration, fibrosis
DMD-4	11 months	Male	Dystrophic process, central nuclei, fiber size variation
DMD-5	8.0	Male	Mild dystrophy, endomysial fibrosis, larger fibers
DMD-6	7.0	Male	Mid-stage severe dystrophy, endomysial fibrosis, failed regeneration